An Enhanced Assumed Strain (EAS) Solid Element for Nonlinear Implicit Analyses

Fredrik Bengzon†, Thomas Borrvall† and Ushnish Basu††
†*DYNAmore Nordic AB*
††*Livermore Software Technology Corporation (LSTC)*

Abstract

Historically, the importance of computational efficiency in explicit analysis has driven the element development in LS-DYNA® [1,2] towards fast and sufficiently accurate formulations. Single point integrated elements with stabilization are well established techniques in this area. The recent growth of implicit analysis has led to a demand of increased accuracy of the element response, and consequently more sophisticated formulations have been introduced in recent years. While high order elements provide a better response, low order elements remain popular due to their simplicity and robustness. An area that has not yet been exploited in LS-DYNA is the family of enhanced assumed strain (EAS) elements, the reason being the computational cost associated with this approach. Solid element 18 is a linear Wilson element based on this technology, but is only available for linear implicit analysis. The goal with this paper is to generalize this to fully nonlinear implicit analysis, and provide information on its merits and drawbacks.

Introduction

Isoparametric Strain Elements

The design of a finite element is essentially the design of its deformation gradient $\boldsymbol{F}$, the mother of all strains. The deformation gradient is in a continuum mechanical context defined as

$$\boldsymbol{F} = \frac{\partial \boldsymbol{x}}{\partial \boldsymbol{X}}$$

where $\boldsymbol{x}$ is the current spatial location for a given reference material coordinate $\boldsymbol{X}$, and is a measure of the stretch and rotation of an infinitesimal line element in the body. Based on $\boldsymbol{F}$, examples of different strain measures are

$$\boldsymbol{\varepsilon} = ln\boldsymbol{F}^T\boldsymbol{F} \qquad \text{(natural strain)}$$
$$\boldsymbol{E} = \frac{1}{2}(\boldsymbol{F}^T\boldsymbol{F} - \boldsymbol{I}) \qquad \text{(Green strain)}$$
$$\boldsymbol{D} = sym\dot{\boldsymbol{F}}\boldsymbol{F}^{-1} \qquad \text{(rate of deformation)}$$
$$\boldsymbol{e} = \frac{1}{2}(\boldsymbol{I} - \boldsymbol{F}^{-T}\boldsymbol{F}^{-1}) \qquad \text{(Almansi strain).}$$

For a given strain measure we can imagine that all possible strains generated by arbitrary deformations constitutes a *strain space* $\mathcal{E}$, so for instance $\boldsymbol{E} \in \mathcal{E}$ if we happen to work with the Green strain measure. Now, when a continuum body is discretized into finite elements, each *element* is in the simplest setting represented by m coordinate points $\boldsymbol{x}_i$ and associated isoparametric shape functions N_i, $i = 1, \dots, m$. The spatial location of a material point in the element is written as

$$\boldsymbol{x} = \boldsymbol{x}_i N_i$$

and a direct application results in

$$\boldsymbol{F} = \boldsymbol{x}_i \frac{\partial N_i}{\partial \boldsymbol{X}}.$$

The consequence of the discretization is that the *numerical* strains using this latter $\boldsymbol{F}$ are restricted to a finite dimensional subspace $\mathcal{E}_h$ of the space of *continuum* strains $\mathcal{E}$, and the *quality* of the element comes down to the richness of this subspace $\mathcal{E}_h \subset \mathcal{E}$. To this end, for a given level of discretization h, the subspace is to most extent defined by the choice of shape functions N_i. It is for instance known that high order polynomials tend to improve the situation as they appropriately enlarge the space of strains.

Considering low order hexahedral elements, for which the shape functions are the standard tri-linear isoparametric shape functions, the methodology presented above inevitably leads to *locking* phenomena, i.e., the element becomes too stiff. In short, this is explained by the element's inability to represent a physical deformation mode without exhibiting spurious strain. Typically, a pure bending deformation is accompanied with either excessive volumetric or shear strain that absorbs energy and stiffens the response. To use a phrasing that reconnects to the discussion above, the strain space $\mathcal{E}_h$ is too small.

Assumed Strain Elements

A way to deal with locking is to augment the deformation gradient based on reasonable assumptions, leading to an *assumed strain element* with deformation gradient $\boldsymbol{F}_{as}$. There are restrictions associated with such a modification, a crucial one is to maintain frame invariance by making sure that the assumed velocity gradient $\boldsymbol{L}_{as} = \dot{\boldsymbol{F}}_{as}\boldsymbol{F}_{as}^{-1}$ is skew-symmetric whenever elements undergo rigid body motion. A not so severe restriction is that the element satisfies various *patch tests* commonly found in the literature. A first example of such an approach is to assume that the deformation gradient is constant in an element and given as either its value in the center, $\boldsymbol{F}_{as} = \boldsymbol{F}_0$, or its integrated mean, $\boldsymbol{F}_{as} = \overline{\boldsymbol{F}}$. This will on the one hand alleviate locking but on the other render an incomplete element in the sense that non-rigid deformation modes won't generate strains, i.e., the symmetric part of $\boldsymbol{L}_{as}$ is zero. Such elements require artificial (hourglass) stabilization and are available as the type 1 element in LS-DYNA. A complete element is resulted from assuming that only the volumetric part of the deformation gradient is constant, and the deviatoric part unaffected. This is the so called *selective reduced integration element* available as type 2 in LS-DYNA. We either have $\boldsymbol{F}_{as} = (J_0/J)^{1/3}\boldsymbol{F}$ or $\boldsymbol{F}_{as} = (\bar{J}/J)^{1/3}\boldsymbol{F}$ depending on the choice of averaging, where $J = det\boldsymbol{F}$ is the jacobian. The choice of $\bar{J}$ is preferred over J_0 as this element satisfies the patch test, the other does not. This element alleviates volumetric locking but still exhibits stiff behavior in shear, in particular for elements with poor aspect ratio. A heuristic approach to deal with the latter is presented in [3], and the corresponding element is available as types -1 and -2 in LS-DYNA. Those elements do not satisfy the patch test.

Enhanced Assumed Strain Elements

Pioneered by Juan Simo and co-workers in the late 80's and early 90's, the concept of *enhanced* assumed strain elements emerged in the finite element community [4]. For these elements the deformation gradient is modified by adding an enhanced contribution $\boldsymbol{F}_e$

$$\boldsymbol{F}_{eas} = \boldsymbol{F} + \boldsymbol{F}_e.$$

The enhanced contribution $\boldsymbol{F}_e$ is in turn a function of an independent field $\boldsymbol{\alpha}$ that can be seen as representing deformation modes in which the element needs to be relaxed, i.e., this is a way to enlarge the strain space. The presence of $\boldsymbol{\alpha}$ implies the existence of a work conjugate field $\boldsymbol{f}_\alpha$, and appropriate application of the virtual work principle results in that an additional set of equations, $\boldsymbol{f}_\alpha = \boldsymbol{0}$, needs to be solved. Fortunately, $\boldsymbol{\alpha}$ is assumed discontinuous over element boundaries, which means that this compatibility equation can be solved locally for each element and the size of the global system of equations is thus unaffected. Nevertheless, solving many local sets of nonlinear equations adds a significant overall cost to evaluating the nodal forces, and is the main reason why it has not been given much attention in an *explicit* finite element context. For *implicit* time integration the story may be told differently, the price of spending more time in element routines may give payback in the currency of better results and larger time steps. The purpose of this paper is to investigate this potential.

Theory

General

A framework for the design of enhanced assumed strain elements sufficient for satisfying frame invariance and patch tests was introduced by Simo and Rafai [4]. Within this framework, Simo et.al. [5] developed some specific elements with interesting properties, and this is an attempt to summarize the equations behind one of these. For this we treat a single element occupying a region Ω in space, and emphasize that the notation used from hereon is independent of the notation used in previous sections.

Let $\boldsymbol{x}$ denote the coordinate vector for the nodes in the current configuration, $\boldsymbol{x}_n$ the coordinate vector in the previous (converged) configuration and $\boldsymbol{x}_0$ the coordinate vector in the reference configuration. We then let $\boldsymbol{u} = \boldsymbol{x} - \boldsymbol{x}_n$ and $\boldsymbol{v} = \boldsymbol{u}/\Delta t$ be the displacement and velocity vectors, respectively, where Δt is the time step. All vectors mentioned so far are of dimension 24, 8 nodes times 3 degrees of freedom per node. The element is characterized by a vector $\boldsymbol{\alpha}$ of dimension 12 representing the enhanced deformation modes, and we likewise use $\boldsymbol{\alpha}_n$ to denote its value in the previous configuration, and use $\Delta\boldsymbol{\alpha} = \boldsymbol{\alpha} - \boldsymbol{\alpha}_n$ for its increment. There are 4 enhanced modes, each represented by a triplet $\boldsymbol{\alpha}_i, i = 1, \dots, 4$.

The enhanced deformation gradient is denoted $\boldsymbol{F} = \boldsymbol{F}(\boldsymbol{x}, \boldsymbol{\alpha})$, and the constitutive law takes a strain measure as input to compute or increment the resulting Cauchy stress $\boldsymbol{\sigma}$. Through a work principle, where we use δ_1 to denote the first variation, the identification of $\boldsymbol{f}_x$ and $\boldsymbol{f}_\alpha$ can be made by the relation

$$\delta_1\boldsymbol{x}^T\boldsymbol{f}_x + \delta_1\boldsymbol{\alpha}^T\boldsymbol{f}_\alpha = \int_\Omega (\delta_1\boldsymbol{F}\boldsymbol{F}^{-1}) : \boldsymbol{\sigma} d\Omega.$$

The stiffness matrix terms can likewise be identified through the second variation δ_2 of this work principle

$$\delta_1 \boldsymbol{x}^T \frac{\partial \boldsymbol{f}_x}{\partial \boldsymbol{x}} \delta_2 \boldsymbol{x} + \delta_1 \boldsymbol{x}^T \frac{\partial \boldsymbol{f}_x}{\partial \boldsymbol{\alpha}} \delta_2 \boldsymbol{\alpha} + \delta_1 \boldsymbol{\alpha}^T \frac{\partial \boldsymbol{f}_\alpha}{\partial \boldsymbol{x}} \delta_2 \boldsymbol{x} + \delta_1 \boldsymbol{\alpha}^T \frac{\partial \boldsymbol{f}_\alpha}{\partial \boldsymbol{\alpha}} \delta_2 \boldsymbol{\alpha} = \cdots =$$
$$= \int_\Omega \left(\delta_2 \delta_1 \boldsymbol{F}\boldsymbol{F}^{-1} + (\delta_2 \boldsymbol{F}\boldsymbol{F}^{-1})^T (\delta_1 \boldsymbol{F}\boldsymbol{F}^{-1}) \right) : \boldsymbol{\sigma} d\Omega + \int_\Omega (\delta_1 \boldsymbol{F}\boldsymbol{F}^{-1}) : \boldsymbol{C} : (\delta_2 \boldsymbol{F}\boldsymbol{F}^{-1}) d\Omega.$$

Worth noticing here is that for this relation to hold, $\boldsymbol{C}$ is the constitutive modulus relating the *Truesdell* rate of Cauchy stress to the rate-of-deformation. Following Simo et.al. [5], all integrals above are numerically integrated using a 9 point integration scheme.

The first of the force vectors, $\boldsymbol{f}_x$, should balance the other forces in the problem, while the second, $\boldsymbol{f}_\alpha$, should solve the compatibility equation $\boldsymbol{f}_\alpha = \boldsymbol{0}$ for the current value of $\boldsymbol{\alpha}$. For this, we use a Newton method and the corresponding Hessian $\frac{\partial \boldsymbol{f}_\alpha}{\partial \boldsymbol{\alpha}}$. The elimination of $\boldsymbol{\alpha}$ on the element level requires that the global tangent stiffness matrix is condensated accordingly, we have

$$\boldsymbol{K}_x = \frac{d\boldsymbol{f}_x}{d\boldsymbol{x}} = \frac{\partial \boldsymbol{f}_x}{\partial \boldsymbol{x}} + \frac{\partial \boldsymbol{f}_x}{\partial \boldsymbol{\alpha}} \frac{\partial \boldsymbol{\alpha}}{\partial \boldsymbol{x}}$$

where $\frac{\partial \boldsymbol{\alpha}}{\partial \boldsymbol{x}}$ is obtained through the variation of the compatibility equation

$$\frac{d\boldsymbol{f}_\alpha}{d\boldsymbol{x}} = \frac{\partial \boldsymbol{f}_\alpha}{\partial \boldsymbol{x}} + \frac{\partial \boldsymbol{f}_\alpha}{\partial \boldsymbol{\alpha}} \frac{\partial \boldsymbol{\alpha}}{\partial \boldsymbol{x}} = \boldsymbol{0} \;\Rightarrow\; \frac{\partial \boldsymbol{\alpha}}{\partial \boldsymbol{x}} = -\left(\frac{\partial \boldsymbol{f}_\alpha}{\partial \boldsymbol{\alpha}} \right)^{-1} \frac{\partial \boldsymbol{f}_\alpha}{\partial \boldsymbol{x}}$$

so

$$\boldsymbol{K}_x = \frac{\partial \boldsymbol{f}_x}{\partial \boldsymbol{x}} - \frac{\partial \boldsymbol{f}_x}{\partial \boldsymbol{\alpha}} \left(\frac{\partial \boldsymbol{f}_\alpha}{\partial \boldsymbol{\alpha}} \right)^{-1} \frac{\partial \boldsymbol{f}_\alpha}{\partial \boldsymbol{x}}.$$

Specifics

The assumed deformation gradient can be expressed as

$$\boldsymbol{F} = \left\{ \boldsymbol{x}_i \frac{\partial N_i}{\partial \boldsymbol{\xi}} \boldsymbol{J}_\xi^{-1} \right\}_{Galerkin} + \left\{ \boldsymbol{\alpha}_j \left(\frac{J_0}{J_\xi} \right) \frac{\partial \widetilde{N}_j}{\partial \boldsymbol{\xi}} \boldsymbol{J}_0^{-1} \right\}_{Wilson} + \left\{ \left[\left(\frac{J_0}{J_\xi} \right) \frac{\partial \widetilde{N}_4}{\partial \boldsymbol{\xi}} \boldsymbol{J}_0^{-1} \boldsymbol{\alpha}_4 \right] \boldsymbol{x}_i \frac{\partial N_i}{\partial \boldsymbol{\xi}} \Big|_0 \boldsymbol{J}_0^{-1} \right\}_{Volume},$$

where the first term is the standard Galerkin term and the remaining are the enhanced contributions. We here use $\boldsymbol{x}_i$ to denote the coordinate vector of node $i, i = 1, \ldots, 8$, and $\boldsymbol{\alpha}_j$ to denote the jth enhanced variable, $j = 1 \ldots, 4$. All these vectors are column vectors of dimension 3. The shape functions associated with the enhanced contributions are the so called Wilson incompatible shape functions

$$\widetilde{N}_j = \frac{1}{2}(\xi_j^2 - 1),$$

for $j = 1,2,3$, to relax bending deformations, and a function intended to alleviate volumetric locking

$$\widetilde{N}_4 = \xi_1\xi_2\xi_3.$$

We also use $\boldsymbol{J}_\xi/J_\xi$ and $\boldsymbol{J}_0/J_0$ to denote the jacobian matrix/determinant between the iso-parametric and reference domains, and subscript 0 means that a quantity is evaluated at the center point of the domain. Noting that $\frac{\partial(^\circ)}{\partial\boldsymbol{\xi}}$ is a row vector of dimension 3, all operations in the expression for $\boldsymbol{F}$ can be viewed as standard matrix notation. The variation operator is denoted δ_1, and this applied on $\boldsymbol{F}$ becomes

$$\delta_1\boldsymbol{F} = \delta_1\boldsymbol{x}_i\left\{\frac{\partial N_i}{\partial\boldsymbol{\xi}}\boldsymbol{J}_\xi^{-1} + \left[\left(\frac{J_0}{J_\xi}\right)\frac{\partial\widetilde{N}_4}{\partial\boldsymbol{\xi}}\boldsymbol{J}_0^{-1}\boldsymbol{\alpha}_4\right]\frac{\partial N_i}{\partial\boldsymbol{\xi}}\bigg|_0\boldsymbol{J}_0^{-1}\right\} + \delta_1\boldsymbol{\alpha}_j\left\{\left(\frac{J_0}{J_\xi}\right)\frac{\partial\widetilde{N}_j}{\partial\boldsymbol{\xi}}\boldsymbol{J}_0^{-1}\right\}$$
$$+\left[\left(\frac{J_0}{J_\xi}\right)\frac{\partial\widetilde{N}_4}{\partial\boldsymbol{\xi}}\boldsymbol{J}_0^{-1}\delta_1\boldsymbol{\alpha}_4\right]\left\{\boldsymbol{x}_i\frac{\partial N_i}{\partial\boldsymbol{\xi}}\bigg|_0\boldsymbol{J}_0^{-1}\right\},$$

where sum over i is from 1 to 8, while sum over j is from 1 to 3. Because of the product term involving $\boldsymbol{x}$ and $\boldsymbol{\alpha}$, the second variation is non-vanishing, denoting this δ_2 we have

$$\delta_2\delta_1\boldsymbol{F} = \left\{\left[\left(\frac{J_0}{J_\xi}\right)\frac{\partial\widetilde{N}_4}{\partial\boldsymbol{\xi}}\boldsymbol{J}_0^{-1}\delta_1\boldsymbol{\alpha}_4\right]\delta_2\boldsymbol{x}_i\frac{\partial N_i}{\partial\boldsymbol{\xi}}\bigg|_0\boldsymbol{J}_0^{-1} + \left[\left(\frac{J_0}{J_\xi}\right)\frac{\partial\widetilde{N}_4}{\partial\boldsymbol{\xi}}\boldsymbol{J}_0^{-1}\delta_2\boldsymbol{\alpha}_4\right]\delta_1\boldsymbol{x}_i\frac{\partial N_i}{\partial\boldsymbol{\xi}}\bigg|_0\boldsymbol{J}_0^{-1}\right\}.$$

These variations can be inserted into the expressions for nodal forces and stiffnesses in previous sections and completes the basic theory of the element.

Modifications

Two modifications to the equations given above were done.

In order to alleviate volumetric locking for distorted meshes in the incompressible limit, the following modification of the Galerkin term of the deformation gradient is used,

$$\boldsymbol{F}_{Galerkin} = \boldsymbol{x}_i\frac{\partial N_i}{\partial\boldsymbol{\xi}}\bigg|_0\boldsymbol{J}_0^{-1} + \boldsymbol{x}_i\boldsymbol{\gamma}_i\left(\frac{J_0}{J_\xi}\right)\frac{\partial\boldsymbol{\mathcal{H}}}{\partial\boldsymbol{\xi}}\boldsymbol{J}_0^{-1},$$

where $\boldsymbol{\gamma}_i$ are the familiar γ-vectors (row vector of size 4 for each i) and $\boldsymbol{\mathcal{H}} = (\xi_2\xi_3 \quad \xi_1\xi_3 \quad \xi_1\xi_2 \quad \xi_1\xi_2\xi_3)^T$ the associated hourglass functions commonly used in the representation of low order hexahedral elements. The justification behind this modification comes from studying the incompressibility constraint $\boldsymbol{I}:\delta_1\boldsymbol{F} = 0$ to see that nonzero deformations are trivially allowed with this modification, a discussion can be found in [5].

To suppress known numerical instabilities for highly compressive deformations, the theory above is applied to the *incremental* deformation gradient $\Delta\boldsymbol{F}$. To be specific, the total deformation gradient $\boldsymbol{F}$ is given by

$$\boldsymbol{F} = \Delta\boldsymbol{F}\boldsymbol{F}_n$$

where $\boldsymbol{F}_n$ is the deformation gradient in the previous time step, treated as an internal history variable, and the enhanced assumed strain theory is applied to $\Delta\boldsymbol{F}$ using the last known configuration as the reference configuration.

Examples

To validate the element we present and discuss some examples.

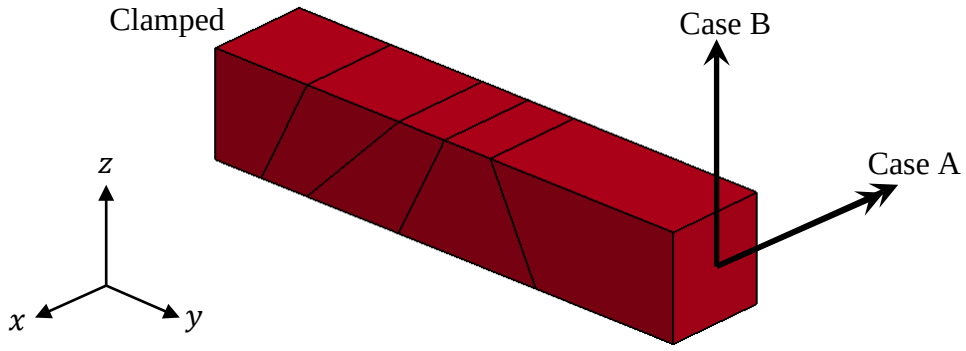

Figure 1 Distorted beam with load cases

Distorted Beam

The beam shown in Figure 1 is equipped with an elastic material, $E = 1500$ and $\upsilon = 0.25$, and is an example to test the element sensitivity to a distorted mesh. The beam, of dimension $2 \times 2 \times 10$, is clamped at one end, and on the other a bending torque of 40 (case A) and a transverse load of 6 (case B) is applied. The analytical end tip displacement for case A is 1 and for case B 1.026 and Table 1 summarizes the numerical results.

Table 1 Z-displacement for distorted beam

Element Type	Case A	Case B
1 – Belytchko-Bindeman HG	0.780	0.829
1 – Cosserat HG	0.976	1.002
2 – S/R integration	0.782	0.869
18 – EAS	0.911	0.934
24 – Quadratic	0.989	1.008

Not surprisingly the high order element provides the most accurate response, followed by the Cosserat element. The Cosserat element is a low order element with a sophisticated hourglass treatment accounting for the mesh distortion in the reference configuration, which may explain the good result. Among the other elements the EAS element presented here is most accurate, and the results compare well with those in [6]. In general low order elements seem sensitive to the shape of the elements, and even though the Cosserat element performs quite well it is still an hourglass element and may not exhibit correct stress response for larger deformations.

Near-Incompressible Block

The block shown in Figure 2 is also equipped with an elastic material, but nearly incompressible with $\upsilon = 0.4999$, and $E = 210000$. This is an example to test how stiff the element as well as its performance under constrained conditions. The block has a height of 50 and length and width 100, but only one quarter is meshed due to symmetry. The base of the block is clamped and a uniform distributed pressure of 250, acting on an area of 20×20, is applied in the center of the top. Two meshes are tested, both with $5 \times 5 \times 5$ elements, but one structured (case A) and one slightly distorted (case B). The vertical displacement of the top center node is summarized in Table *2* along with results from [6]. In comparison, the EAS element performs well, and has a reasonable resistance against mesh distortion.

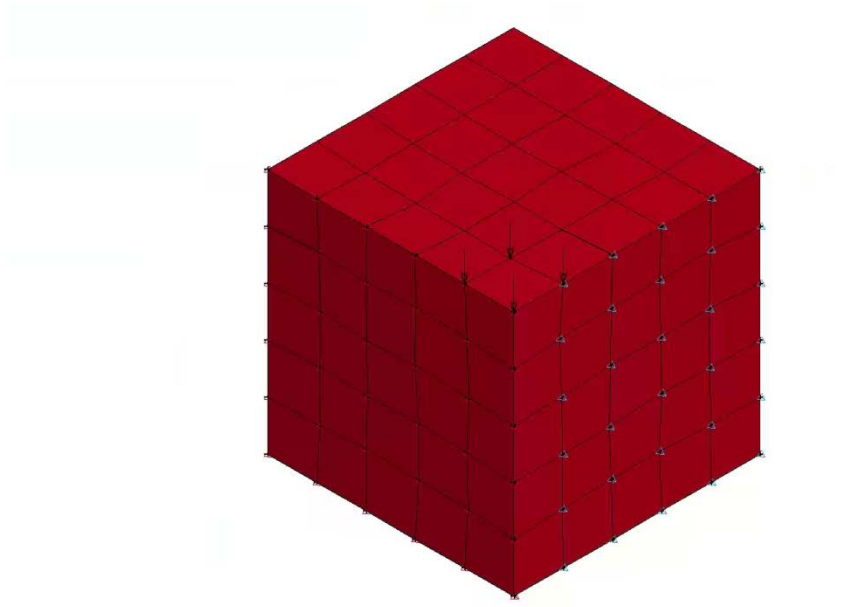

Figure 2 Near-incompressible block subject to a pressure load

Table 2 Z-displacement for near-incompressible block

Element Type	Case A	Case B
1 – Belytschko-Bindeman HG	-1.905e-2	-1.914e-2
2 – S/R integration	-1.966e-2	-1.972e-2
18 – EAS	-1.892e-2	-1.834e-2
Reference [6]	-1.892e-2	-1.840e-2

A shortcoming of EAS methods is that they may exhibit instabilities in a state of finite deformation [7], often under non-linear or severely constrained conditions. Figure 3 depicts one such situation and shows a cube equipped with an elasto-plastic material deforming under compression. After a while hour-glassing develops in the compressed region and convergence breaks down.

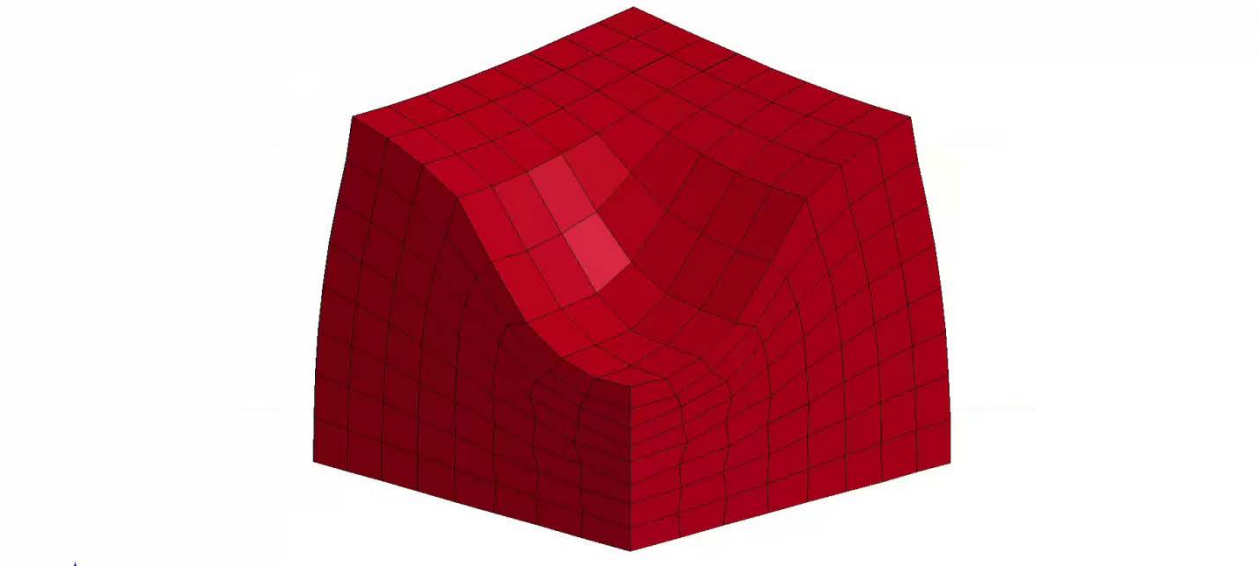

Figure 3 Hourglass instability in the EAS element

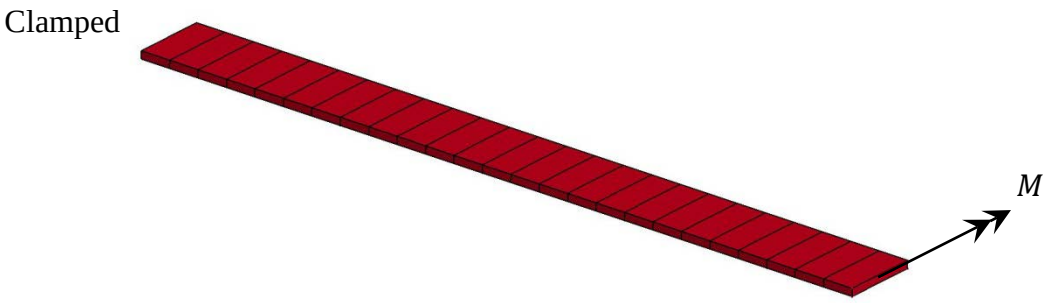

Figure 4 Straight cantilever beam subjected to moment

Nonlinear Cantilever Beam

A straight cantilever beam with dimensions $H \times B \times L = 0.1 \times 1 \times 10$ is discretized into 25 elements along its length, see Figure 4. It is clamped at one end, and a moment $M = \frac{EBH^3\pi}{6L}$ is applied at the other that analytically will transform the beam into a perfect cylinder. The material is hyperelastic with $E = 12000000$ and zero Poisson ratio.

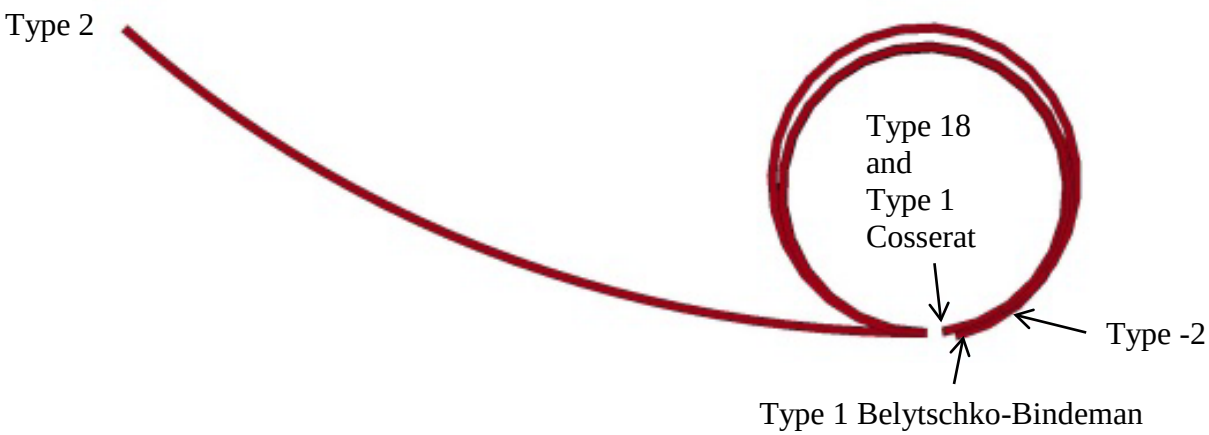

Figure 5 Final configuration of cantilever beam

Figure 5 shows the deformed configurations for some element types. Noticable is that the fully integrated element type 2 locks in shear for this element geometry and load case, something that is alleviated by using type -2. The latter is still not as good as the others, presumably because only one element through the thickness is used and the constant pressure profile prohibits a proper bending response. The EAS element is together with the Cosserat formulation giving the best result, albeit not perfect.

Summary

A nonlinear extension of the linear type 18 element in LS-DYNA has been implemented and presented. It is based on an enhanced assumed strain theory which is renowned for accurate response but suffering from computationally intense calculations. The main intention is to offer this element as part of the nonlinear implicit solver, for which the computational expense in element routines is not as devastating as in explicit analysis. At the time of writing, the element routines are not optimized for speed and the overhead compared to other fully integrated elements is in the order of 10 times, but there is good hope for improvements on that note. The examples presented are fairly simple and serves the purpose of comparing the element to other available formulations, we are yet to exercise it in more complex situations but hope this will be done in the near future.

References

1. LS-DYNA Keyword Manual, Volumes I-II, Livermore Software Technology Corporation.
2. T. Erhart, *Review of solid element formulations in LS-DYNA*, LS-DYNA Forum, October 12-13, 2011, Filderstadt, Germany.
3. T. Borrvall, *A heuristic attempt to reduce transverse shear locking in fully integrated hexahedra with poor aspect ratio*, Proc. 7th European LS-DYNA Conference, Salzburg, 2009.
4. J.C. Simo and M.S. Rafai, *A class of mixed assumed strain methods and the method of incompatible modes*, Int. J. Numer. Methods Eng. 29 (1990) pp. 1595-1638.
5. J.C. Simo, F. Armero and R.L. Taylor, *Improved versions of assumed enhanced strain tri-linear elements for 3D finite deformation problems*, Comput. Methods in Appl. Mech. Eng. 110 (1993) pp. 359-386.
6. P.M.A. Areias, J.M.A. César de Sá, C.A. Conceição António and A.A. Fernandez, *Analysis of 3D problems using a new enhanced strain hexahedral element*, Int. J. Numer. Methods Eng. 58 (2003) pp. 1637-1682.
7. P. Wriggers, *Nonlinear Finite Element Methods*, Springer Verlag (2008).